Journal of Comparative Pathology

Novel dermatitis and relative viral nucleic acid tissue loads in a fin whale (Balaenoptera physalus) with systemic cetacean morbillivirus infection

--Manuscript Draft--

Manuscript Number:	
Article Type:	Short Communication
Keywords:	cetacean morbillivirus; dermatitis; fin whale; viral load
Corresponding Author:	Mark Patrick Dagleish, BVM&S, PhD, MRCVS, FRCPath Moredun Research Institute Edinburgh, UNITED KINGDOM
First Author:	Mark Patrick Dagleish, BVM&S, PhD, MRCVS, FRCPath
Order of Authors:	Mark Patrick Dagleish, BVM&S, PhD, MRCVS, FRCPath
	Adele Perri, BSc.
	Madeleine Maley, BSc.
	Keith Ballingall, BSc. PhD
	Johanna Louise Baily, DVM, PhD
	Nicholas John Davison, MSc
	Andrew Brownlow, BVM&S, PhD
	Mara Rocchi, DVM, PhD
Abstract:	Summary Cetacean morbilliviruses (CeMV) are significant causes of mortality affecting many cetacean species in epizootics and smaller outbreaks. Despite skin lesions being prominent in seals and terrestrial animals, including humans, affected by other morbilliviruses, they have not been reported in CeMV-infected cetaceans. Here we report CeMV-associated skin lesions in a fin whale (Balaenoptera physalus) with sub-acute, systemic CeMV infection that live-stranded in Scotland, UK. Grossly, the skin was sloughing in large sheets, presumed due to autolysis but histological examination showed syncytia formation below the dermo-epidermal junction that were strongly positive for morbillivirus antigen by immunohistochemistry, as were syncytia in other organs. By PCR, the relative load of CeMV-specific RNA was largest in the liver and urinary bladder, even in formalin-fixed, paraffin-wax embedded samples. Levels were low in skin and only detectable in frozen samples. Genetic comparison of the CeMV showed close alignment with isolates from fin whales in the North Atlantic Ocean and the Mediterranean Sea but distinct from the porpoise CeMV clade. These findings show skin samples can be used to diagnose CeMV infection in cetaceans highlighting the potential of ante-mortem sampling to monitor disease in current populations and assessment of changes in host and pathogen genetics.

Accepted refereed manuscript of: Dagleish MP, Perri A, Maley M, Ballingall KT, Baily JL, Davison NJ, Brownlow AC & Rocchi MS (2021) Novel Dermatitis and Relative Viral Nucleic Acid Tissue Loads in a Fin Whale (Balaenoptera physalus) with Systemic Cetacean Morbillivirus Infection. *Journal of Comparative Pathology*, 183, pp. 57-62. https://doi.org/10.1016/j.jcpa.2021.01.005

Novel dermatitis and relative viral nucleic acid tissue loads in a fin whale (*Balaenoptera physalus*) with systemic cetacean morbillivirus infection

[*]M.P. Dagleish, [*]A. Perri, [*]M. Maley, [*]K.T. Ballingall, [*§]J.L. Baily, [†]N.J. Davison, [†]A.C. Brownlow & [*]M.S. Rocchi

[*]*Moredun Research Institute, Pentlands Science Park, Bush Loan, Penicuik, Scotland, EH26 0PZ, UK,* [†]*Scottish Marine Animal Strandings Scheme, SRUC Northern Faculty, An Lòchran, Inverness Campus, Inverness, Scotland, IV2 5NA*

[§]*Present address: Institute of Aquaculture, University of Stirling, Stirling, Scotland, FK9 4LA, UK*

Correspondence to: M. P. Dagleish (e-mail: mark.dagleish@moredun.ac.uk).

Short title: cetacean morbillivirus dermatitis

Key words: cetacean morbillivirus, dermatitis, fin whale, viral load.

Summary

Cetacean morbilliviruses (CeMV) are significant causes of mortality affecting many cetacean species in epizootics and smaller outbreaks. Despite skin lesions being prominent in seals and terrestrial animals, including humans, affected by other morbilliviruses, they have not been reported in CeMV-infected cetaceans. Here we report CeMV-associated skin lesions in a fin whale (*Balaenoptera physalus*) with sub-acute, systemic CeMV infection that live-stranded in Scotland, UK. Grossly, the skin was sloughing in large sheets, presumed due to autolysis but histological examination showed syncytia formation below the dermo-epidermal junction that were strongly positive for morbillivirus antigen by immunohistochemistry, as were syncytia in other organs. By PCR, the relative load of CeMV-specific RNA was largest in the liver and urinary bladder, even in formalin-fixed, paraffin-wax embedded samples. Levels were low in skin and only detectable in frozen samples. Genetic comparison of the CeMV showed close alignment with isolates from fin whales in the North Atlantic Ocean and the Mediterranean Sea but distinct from the porpoise CeMV clade. These findings show skin samples can be used to diagnose CeMV infection in cetaceans highlighting the potential of ante-mortem sampling to monitor disease in current populations and assessment of changes in host and pathogen genetics.

Introduction

Cetacean morbillivirus (CeMV) is a distinct species made up of three well characterised strains named after the species in which they were initially found (porpoise morbillivirus, dolphin morbillivirus [DMV] and pilot whale morbillivirus) plus one recovered later from a Longman's beaked whale (*Indopacetus pacificus*), collectively called CeMV-1. Two more strains, recovered more recently from a Guiana dolphin (*Sotalia guianensis*) and two Indo Pacific bottlenose dolphins (*Tursiops aduncus*), are collectively called CeMV-2 (Van

Bressem *et al*., 2014). It is an unsegmented, linear, negative-sense, single-stranded, RNA virus belonging to the genus *Morbillivirus*, family *Paramyxoviridae*, order Mononegavirales and has been responsible for epizootics in odontocetes and mysticetes (Van Bressem *et al*., 2014) including fin whales (*Balaenoptera physalus*) (Mazzariol *et al*., 2016).

Beffagna *et al*. (2017) suggested that the lack of typical morbillivirus pathology on post-mortem examination in a subset of stranded, CeMV-1 infected, striped (*Stenella coeruleoalba*) and bottlenose (*Tursiops truncatus*) dolphins (Casalone *et al*., 2014) may be due to genomic variations in the virus compared to the CeMV-1 originally detected in previous epizootics in the Mediterranean Sea, which affected mainly striped dolphins and long-finned pilot whales (*Globicephala melas*). They also suggested the genomic variations might have facilitated fin whale infections in the Mediterranean Sea resulting in several cases where CeMV-1 specific RNA was found in the brain, lung and spleen of a stranded neonate and the liver, spleen, lung, lymph nodes and skeletal muscle of older animals (Mazzariol *et al*., 2016). Previous reports of CeMV infection in fin whales have described lesions including non-suppurative encephalitis, 'bronchiolo-interstitial' pneumonia, hepatitis, mild catarrhal enteritis and lymphoid depletion of the spleen and pulmonary and prescapular lymph nodes (Di Guardo *et al*., 2013; Mazzariol *et al*., 2016). Definitive CeMV-related skin lesions have not been reported in cetaceans nor the relative amounts of CeMV specific RNA present in different organs during systemic infection.

Material and Methods

An adult, male fin whale (M37/13) live-stranded in the Cree estuary, Dumfries and Galloway, Scotland, UK (54°52'29.3"N and 4°22'38.8"W) and died within 12 hours of being found. A standardised necropsy was performed 36 hrs after death (Kuiken and Hartman, 1991).

Samples for bacteriology (brain, cerebrospinal fluid (CSF), heart, lung, liver, spleen, kidney, intestine, pulmonary-associated and mesenteric lymph node) were cultured (as detailed in Davison *et al*., 2015).

Tissue samples, including (part brain stem and cerebellum [sampled through the foramen magnum], trachea, lung, myocardium and attached cyst, heart valve, liver, stomach [cardiac region], spleen, three lymph nodes [two pulmonary-associated, one mesenteric], kidney, urinary bladder, testis and skin) were fixed in 10% neutral-buffered formalin and processed routinely through graded alcohols prior to embedding in paraffin-wax. Sections (4 µm) were stained with haematoxylin and eosin (HE) and subjected to immunohistochemistry (IHC) for morbillivirus antigen as described previously (Wessels *et al*., co-submission). Sections were graded for the extent of IHC labelling (0 = absent, 1 = perceptible, 2 = small, 3 = medium, 4 = large and 5 = very large).

Brain and skin samples were frozen (-80°C) and RNA was extracted from these and all formalin-fixed, paraffin wax-embedded (FFPE) tissue samples using the RNeasy kit (Qiagen, Manchester, UK) or RecoverAll™ Total Nucleic Acid Isolation Kit (ThermoFisher, Loughborough, UK), respectively, according to manufacturers' protocols. For CeMV-1 PCR, primers and probes were employed in a one-step RT-qPCR reaction targeting the hypervariable C-terminal domain of the nucleocapsid (N) gene of DMV (Grant *et al*., 2009). The reaction was performed in a final volume of 25 µl containing 12.5 µl of reaction mix with ROX (Invitrogen Superscript III Platinum One-Step Quantitative RT-PCR System), 200 nM of each primer, 240 nM probe, 0.5 µl of SuperScript™ III RT/Platinum™ Taq Mix (Thermofisher) and 2 µl of total nucleic acid. Cycling conditions were: 50°C for 15 minutes followed by 95°C for 2 minutes then 45 cycles each consisting of 95°C for 15s, and 60°C for 1 minute (ABI Prism 7500, Applied Biosciences, ThermoFisher). The fluorescence threshold

was set manually above the background level. Two technical replicates were analysed for each sample. Positive target controls (DMV positive liver sample, sequenced) and no template controls were included in all plates. A second RT-qPCR detecting a mammalian housekeeping gene (β−actin) (as detailed in Thonour *et al*., 2012, with 500 nM primers and 200 nM probe) was performed using the above conditions to confirm validity and suitability of extracted nucleic acids. Positive results, expressed as CT (cycle threshold) values indicating the number of cycles required for the fluorescent signal to cross the threshold (i.e. exceed background level), are inversely proportional to the amount of target nucleic acid present.

Total RNA extracted from frozen samples of brain and skin was subjected to RT-PCR amplification of the CeMV-Hemagglutinin binding protein gene, using DMV-F10 and DMV-R10 primers as described by Mazzariol *et al*. (2016). A 718 bp PCR fragment was purified followed by bidirectional Sanger sequencing using the DVM-10 primers. A full length consensus sequence was generated from independent PCR fragments amplified from RNA isolated from brain and skin tissues using SeqMan Pro 15 software within the DNAstar Lasergene package. Sequence identity was confirmed and similarity to other CeMV-H gene sequences was determined by a BLAST search of the NCBI nucleotide database.

A maximum likelihood phylogenetic tree predicting the relationship between closely related CeMV-H gene sequences was constructed in IQ-TREE (Trifinopoulos *et al*., 2016) using a multiple alignment generated using CLUSTAL Omega (Sievers *et al*., 2011). The Rinderpest morbillivirus H gene (Accession MN632637) was included in the alignment to provide a root for the tree. The model selection tool (Kalyaanamoorthy *et al*., 2017) within IQ-TREE was used to select the optimum substitution models, prior to phylogenetic tree estimation. The

optimum substitution model selected for the CeMV sequences was the Kimura 3 parameter model (K3P, Kimura, 1980). Tree topology was tested with 10,000 bootstrap replicates using the ultrafast bootstrap method of Minh *et al*. (2013). The tree was visualised and prepared for publication using Dendroscope 3 (Huson and Scornavacca, 2012).

Results

The animal measured 1,755 cm from tip of upper jaw to fluke notch; the girth measurement immediately rostral to the dorsal fin was 490 cm. The mean of three standard blubber thickness measurements (immediately rostral to the dorsal fin at the dorsal, lateral and ventral aspects) was 57mm. This and reduced mass of the longissimus dorsi muscles indicated poor nutritional condition. Mild excoriations of the fins and fluke (presumed due to live-stranding process), skin sloughing in large sheets (initially presumed autolysis) and opacity of the lens in the left eye were seen but no indication of entanglement. Fluid was present in the nasal cavity and the trachea (presumed seawater) with large amounts of stable foam present in the bronchi. The lungs were congested equally and fluid oozed from the cut surface of the parenchyma. The pulmonary-associated lymph nodes were deep red with dark red-black centres on sectioning. A single, smooth parasitic cyst was present in the myocardium of the left ventricle. The fundic stomach contained several full thickness ulcers (10-155 mm diameter) and the entire gastro-intestinal tract was empty. Liver and kidneys were yellow and the urinary bladder contained a small amount of red-tinged translucent fluid. Bacteriology revealed only post mortem invaders.

Histological examination showed the tracheal, bronchial and bronchiolar sub-mucosa contained large numbers of syncytia, lymphocytes and macrophages (Figure 1), and a similar infiltration was present in the sub-serosa. Large amounts of bile were present in the hepatic

bile ducts. Large numbers of lymphocytes, macrophages and syncytia infiltrated the hepatic parenchyma, sub-mucosa of the stomach, renal cortico-medullary region and formed a band within the urinary bladder detrusor muscle. The spleen was devoid of peri-arteriolar lymphoid sheaths, the red pulp severely depleted of erythrocytes and an inflammatory cell infiltrate similar to that in the other tissues was present primarily in the sub-capsular and trabecular regions. The paracortices of all lymph nodes were mild-moderately depleted of lymphocytes and contained, variably, small to large numbers of syncytia. The dermis of the skin contained a medium to large number of lymphocytes, macrophages and syncytia (Figure 2). A small number of randomly scattered mononuclear glial foci within the caudal medulla oblongata.

Immunohistochemistry for morbillivirus antigen showed intense cytoplasmic labelling in all tissues except the heart, which was devoid of labelling. Principally, syncytia were labelled (Figures 1 and 3, Table 1), except in the medulla oblongata where neurones and their processes were positive but the cerebellum was devoid of labelling. All negative control preparations were devoid of labelling.

Most FFPE tissues were CeMV RNA positive but relative levels varied with the largest amounts in the urinary bladder (CT 22.0) and liver (CT 22.4) but none in the heart, skin or cerebellum (Table 1). Frozen medulla oblongata contained relatively large amounts of CeMV-specific RNA (CT 25.2) whereas frozen skin contained only small amounts (CT 40.2, Table 1). A definitive diagnosis of severe, sub-acute, systemic CeMV-1 infection was made.

CeMV-1 was confirmed by sequence analysis of the morbillivirus H-gene fragment amplified independently from brain and skin tissue. After removal of the primer sequences, the

remaining 678 bp sequence was submitted to the European nucleotide archive (Accn. LR877357). Pairwise comparison with a CeMV-1 sequence derived from a fin whale from Denmark (Accn. MH430939) identified two synonymous substitutions while comparison with a Mediterranean fin whale sequence (Accn. MH430938) also identified two substitutions, one was identical to the Danish sequence while the second was unique and non-synonymous. Phylogenetic analysis of all CeMV-H gene sequences in the NCBI database indicated a high degree of conservation between viruses isolated from different cetacean species. However, two distinct virus clades were identified, one included North Atlantic and Mediterranean whales and dolphins while the second included North Atlantic porpoises (Figure 4).

Discussion

Although not the first case of CeMV in a fin whale, this is the first report of skin lesions definitively co-localised with CeMV-antigen in cetaceans. Gross skin lesions suspicious of CeMV were suspected in Guiana dolphins (*Sotalia guianensis*) (Flach *et al*., 2019) but never proven, and an extensive review of cetacean skin lesions failed to suggest any link with CeMV (van Bressem *et al*., 2015). Conversely, seals with phocine distemper virus (PDV), which is very closely related to canine distemper virus (CDV) and occasionally presents with skin lesions, showed epidermal and follicular hyperplasia, hyperkeratosis, necrosis and morbillivirus-antigen IHC-positive syncytia (Lipscombe *et al*., 2001). Measles virus, the morbillivirus type species, causes skin lesions that coincide with the formation of large numbers of syncytia (Griffin, 2007). As syncytia are present in cetaceans with CeMV it is surprising skin lesions have not been reported previously. These differences may be due to known genetic variations in cetacean signalling leukocyte adhesion molecules (SLAM/F1) to which CeMV binds (Shimizu *et al*., 2013) or, possibly, the presence or absence of poliovirus

receptor-like 4 (PVRL4/nectin-4) that is expressed in epithelial cells to which morbilliviruses bind (Noyce *et al*., 2011).

The relative amounts of CeMV-1 RNA in different tissues during systemic infection have not been reported previously. Typically, in the per-acute stage morbilliviruses infect and replicate in the respiratory mucosa and local immune cells prior to spreading to the immune organs and other viscera in the acute phase. The skin is usually last and this coincides with rash formation in the subacute stage, with the brain variably affected in the subacute-chronic stages (Griffin, 2007). This case highlights the urinary bladder and liver as ideal samples for PCR CeMV diagnosis plus a range of other tissues that even after FFPE, which compromises RNA integrity (Relova *et al*., 2018), remain suitable and when combined with the distribution of CeMV-associated lesions aids accurate disease staging.

Comparative analysis of the CeMV-H-gene identified a high degree of conservation between viruses isolated from cetacean species distributed across the North Atlantic and the Mediterranean. Interestingly, CeMV-H-gene sequence similarity was highest between whales and dolphins compared to CeMV isolated from porpoises, suggesting a more recent or more efficient exchange of CeMV between whales and dolphins compared to porpoises. This may reflect differences in the efficiency of binding of CeMV H protein to its cell surface receptor, a key early event in virus infection (Shimizu *et al.*, 2013).

In conclusion, this case shows cetaceans develop CeMV-associated skin lesions and even somewhat autolytic skin samples are useful for definitive diagnosis. This will be especially useful in large wildlife species as skin is relatively more resistant to autolysis/putrefaction than visceral organs and easier/safer to sample. Furthermore, skin biopsies taken from live

free-ranging animals may be useful for determining morbillivirus status as well as genetic studies of host and pathogen.

Acknowledgments

The authors would like to thank Clare Underwood (Moredun Research Institute) for expert histological and immunohistological preparations. ND and AB are members of the Scottish Marine Animal Strandings Scheme (SMASS) funded by Marine Scotland and Defra, MPD, MM, KB and MR were funded by the Scottish Government, AP by the Erasmus student exchange programme, University of Perugia, Italy and JLB by the Moredun Research Institute and the Royal Zoological Society of Scotland (RZSS).

Table 1: Relative amounts of CeMV-1 specific RNA (CT-value) detected by real-time RT-PCR (the lower the number the greater the amount of RNA) in the various formalin-fixed, paraffin-wax embedded (FFPE) and frozen tissue samples (where stated) and the corresponding results for immunohistochemistry (FFPE only) along with the principal cell type labelled and amount of labelling (0 – 5). UD = undetermined. NA = not applicable.

Figure legends

Figure 1: Histological preparation of tracheal mucosa; note autolytic loss of epithelium (*) and the very large numbers of large syncytia (black arrows) and lymphocytes (yellow arrows) greatly expanding the sub-mucosa. Stain: H&E. Bar = 100µm. Insert. Semi serial section of tracheal mucosa; note extensive cytoplasmic labelling of syncytia for morbillivirus antigen (brown pigment). Immunohistochemistry for morbillivirus antigen counterstained with haematoxylin. Bar = 100µm.

Figure 2: Skin; note syncytia in dermis (yellow arrows) just below the dermo-epidermal junction (black arrows). Stain H&E. Bar = 200µm.

Figure 3: Skin; note syncytia (black arrows) in H&E stained insert (bar = 100µm) and intense labelling of morbillivirus antigen (brown pigment) in the cytoplasm of the syncytia in the main plate (semi-serial section). Immunohistochemistry for morbillivirus antigen counterstained with haematoxylin. Bar = 100µm.

Figure 4: Maximum likelihood phylogenetic tree estimating the relationship between 20 CeMV-H gene sequences. The H gene sequence derived from fin whale M37/13 is marked with an asterisk *. For each sequence, the species of origin, geographic origin and GenBank accession numbers are shown. The Rinderpest morbillivirus H gene (Accession MN632637) roots the tree.

References

Beffagna G, Centelleghe C, Franzo G, Di Guardo G, Mazzariol S (2017) Genomic and structural investigation on dolphin morbillivirus (DMV) in Mediterranean fin whales (*Balaenoptera physalus*). *Scientific Reports*, **7**, 41554; doi: 10.1038/srep41554.

Casalone C, Mazzariol S, Pautasso A, Di Guardo G, Di Nocera F *et al*. (2014) Cetacean strandings in Italy: an unusual mortality event along the Tyrrhenian Sea coast in 2013. *Diseases of Aquatic Organisms*, **109**, 81-86.

Davison NJ, Brownlow A, McGovern B, Dagleish MP, Perrett LL *et al*. (2015) First report of *Brucella ceti*-associated meningoencephalitis in a long-finned pilot whale *Globicephala melas*. *Diseases of Aquatic Organisms*, **116**(3), 237-241.

Di Guardo G, Di Francesco CE, Eleni C, Cocumelli C, Scholl F *et al*. (2013) Morbillivirus infection in cetaceans stranded along the Italian coastline: pathological, immunohistochemical and biomolecular findings. *Research in Veterinary Science*, **94**, 132–137.

Flach L, Alonso MB, Marinho T, Van Waerebeek K, Van Bressem MF (2019) Clinical signs in free-ranging Guiana dolphins *Sotalia guianensis* during a morbillivirus epidemic: case study in Sepetiba Bay, Brazil. *Diseases of Aquatic Organisms*, **133**(3), 175-180.

277 Grant RJ, Banyard AC, Barrett T, Saliki JT, Romero CH (2009) Real-time RT-PCR assays
278 for the rapid and differential detection of dolphin and porpoise morbilliviruses. *Journal of*
279 *Virological Methods*, **156**, 117-123.
280
281 Griffin DE (2007) Measles Virus. In: *Fields Virology*, 5th Edit., DM Knipe, PM Howley,
282 Eds., Lippincott, Williams and Wilkins, Philadelphia, pp. 1551-1585.
283
284 Huson DH, Scornavacca C (2012) Dendroscope 3- An interactive viewer for rooted
285 phylogenetic trees and networks. *Systematic Biology*, **61**, 1061-1067.
286
287 Kalyaanamoorthy S, Minh BQ, Wong TFK, von Haeseler A, Jermiin LS (2017) ModelFinder:
288 Fast model selection for accurate phylogenetic estimates. *Nature Methods*, **14**, 587-589.
289
290 Kimura M (1980) A simple method for estimating evolutionary rates of base substitutions
291 through comparative studies of nucleotide sequences. *Journal of Molecular Evolution*, **16**, 111-
292 120.
293
294 Kuiken T, Hartman MG (1991) Cetacean pathology: Dissection techniques and tissue
295 sampling. In: In: Proc European Cetacean Society 17. European Cetacean Society, Leiden, p
296 1–39.
297
298 Lipscomb TP, Mense MG, Habecker PL, Taubenberger JK, Schoelkopf R (2001) Morbillivirus
299 Dermatitis in Seals. *Veterinary Pathology*, **38**, 724-726.
300

Mazzariol S, Centelleghe C, Beffagna G, Povinelli M, Terracciano G *et al*. (2016) Mediterranean Fin Whales (*Balaenoptera physalus*) threatened by Dolphin Morbillivirus. *Emerging Infectious Diseases*, **22**, 302–305.

Minh BQ, Nguyen MAT, von Haeseler A (2013) Ultrafast Approximation for Phylogenetic Bootstrap. *Molecular Biology and Evolution*, **30**, 1188–1195.

Noyce RS, Bondre DG, Ha MN, Lin LT, Sisson G *et al*. (2011) Tumor cell marker PVRL4 (nectin 4) is an epithelial cell receptor for measles virus. *PLoS Pathogens*, **7**, e1002240.

Relova D, Rios L, Acevedo AM, Coronado L, Perera CL *et al*. (2018) Impact of RNA Degradation on Viral Diagnosis: An Understated but Essential Step for the Successful Establishment of a Diagnosis Network. *Veterinary Science*, **5**(1), 19.

Shimizu Y, Ohishi K., Suzuki, R, Tajima, Y, Yamada, T *et al*. (2013) Amino acid sequence variations of signalling lymphocyte activation molecule and mortality caused by morbillivirus infection in cetaceans. *Microbiology and Immunology*, **57**, 624–632.

Sievers F, Wilm A, Dineen D, Gibson TJ, Karplus K *et al*. (2011) Fast, scalable generation of high-quality protein multiple sequence alignments using Clustal Omega. *Molecular Systems Biology*, **7**:539.

Thonur L, Maley M, Gilray J. Crook T, Laming E *et al*. (2012) One-step multiplex real time RT-PCR for the detection of bovine respiratory syncytial virus, bovine herpesvirus 1 and bovine parainfluenza virus 3. *BMC Veterinary Research*, **8**:37.

Trifinopoulos J, Nguyen L-T, von Haeseler A, Minh BQ (2016) W-IQ-TREE: a fast online phylogenetic tool for maximum likelihood analysis. *Nucleic Acids Research*, **44**, W232-W235.

Van Bressem M.-F, Duignan P, Banyard A, Barbieri M, Colegrove K *et al*., (2014) Cetacean morbillivirus: current knowledge and future directions. *Viruses*, **6**, 5145–5181.

Van Bressem MF, Flach L, Reyes JC, Echegaray M, Santos M *et al*., (2015) Epidemiological characteristics of skin disorders in cetaceans from South American waters. *Latin American Journal of Aquatic Mammals*, **10**, 20−30.

Wessels M, Deaville R, Perkins M, Jepson P, Penrose R *et al*. Novel presentation of DMV-associated encephalitis in a long-finned pilot whale (*Globicephala melas*). *Journal of Comparative Pathology*. Co-submission with this manuscript.

Figure 1

Click here to access/download;Figure;Figure 1.tif

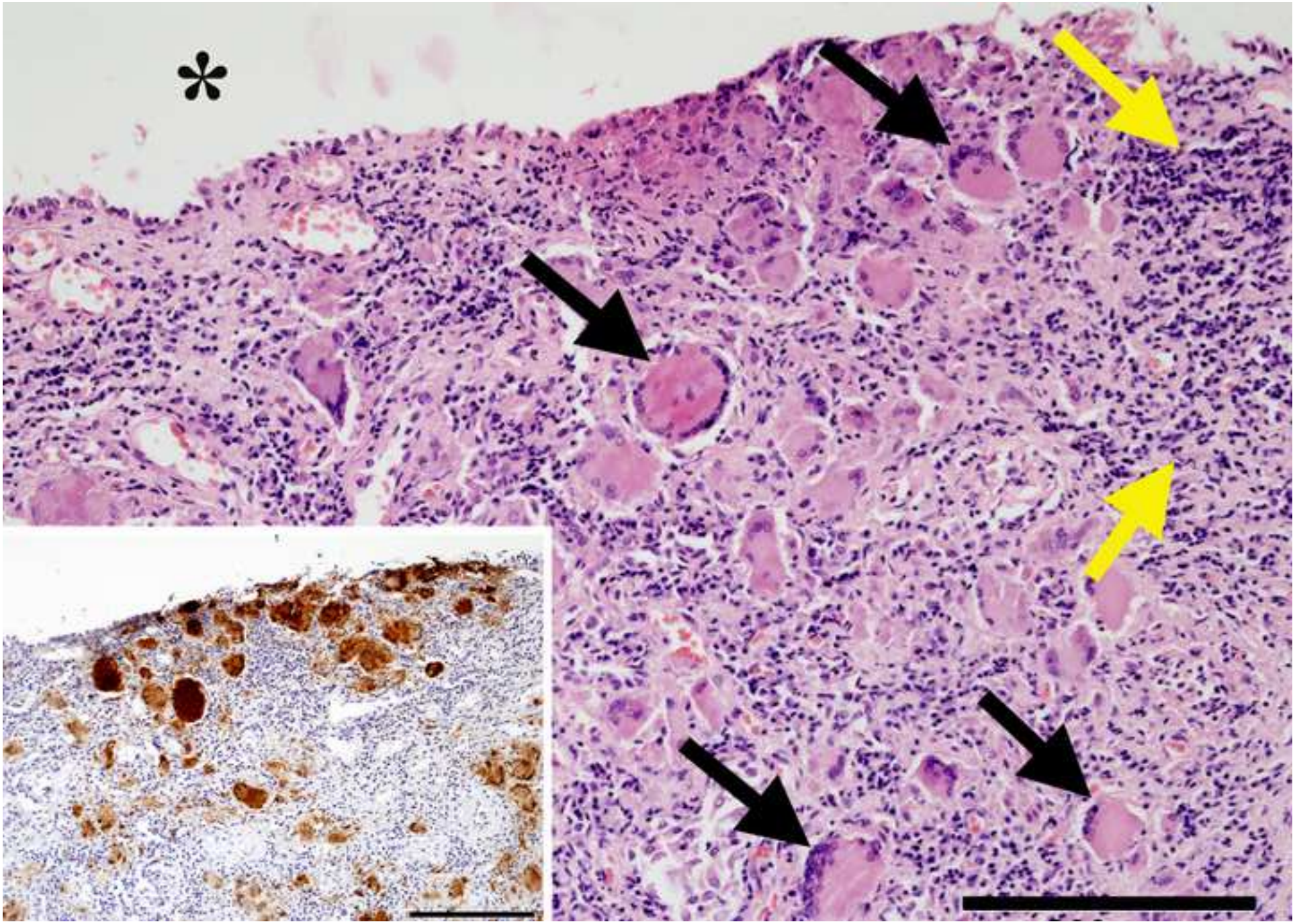

Figure 2

Click here to access/download;Figure;Figure 2.tif

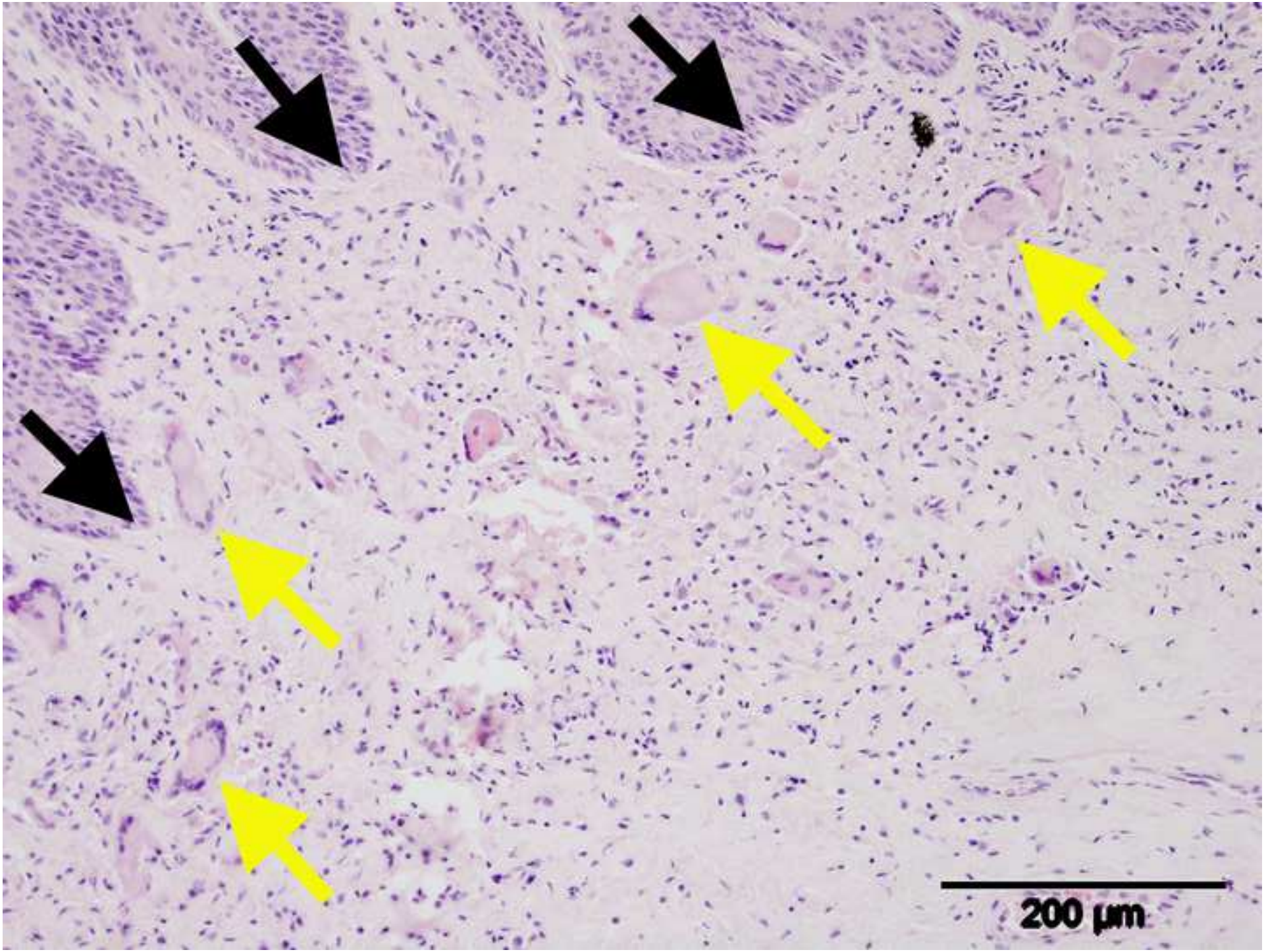

Figure 3

Click here to access/download;Figure;Figure 3.tif

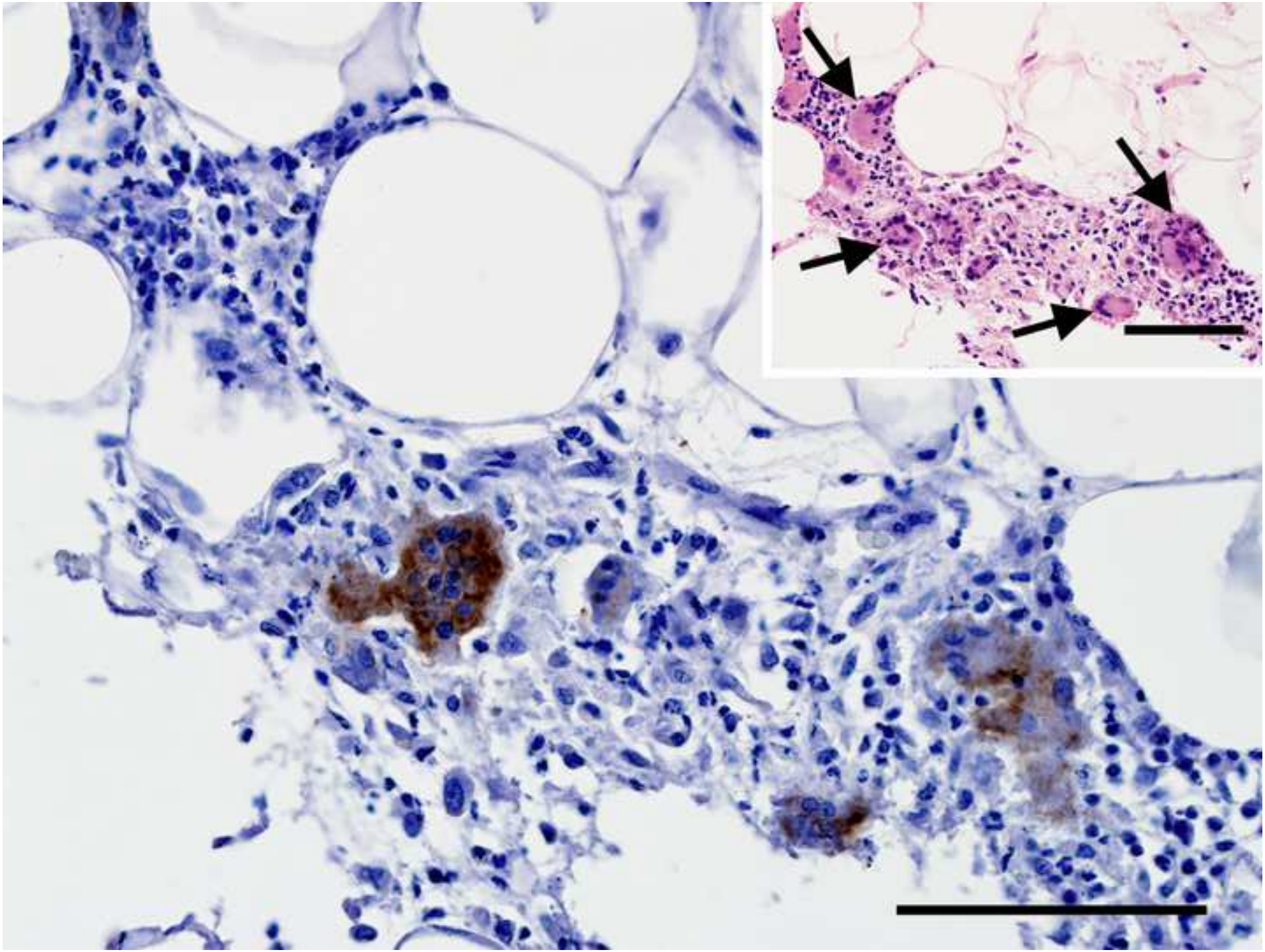

Figure 4

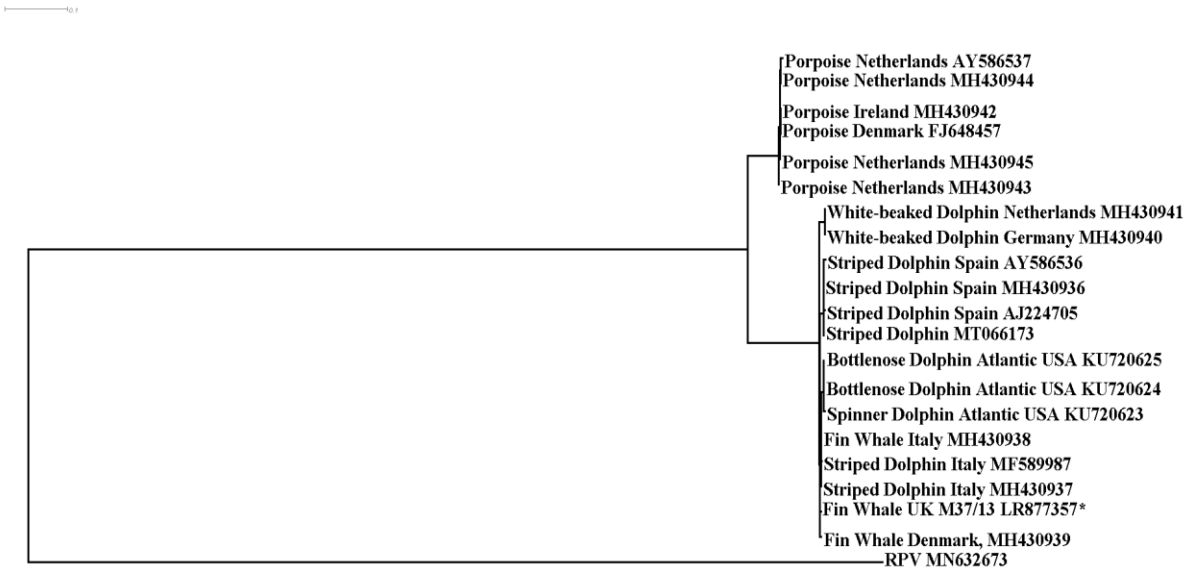
Porpoise Netherlands AY586537
Porpoise Netherlands MH430944
Porpoise Ireland MH430942
Porpoise Denmark FJ648457
Porpoise Netherlands MH430945
Porpoise Netherlands MH430943
White-beaked Dolphin Netherlands MH430941
White-beaked Dolphin Germany MH430940
Striped Dolphin Spain AY586536
Striped Dolphin Spain MH430936
Striped Dolphin Spain AJ224705
Striped Dolphin MT066173
Bottlenose Dolphin Atlantic USA KU720625
Bottlenose Dolphin Atlantic USA KU720624
Spinner Dolphin Atlantic USA KU720623
Fin Whale Italy MH430938
Striped Dolphin Italy MF589987
Striped Dolphin Italy MH430937
Fin Whale UK M37/13 LR877357*
Fin Whale Denmark, MH430939
RPV MN632673

Table 1: Relative amounts of CeMV-1 specific RNA (CT-value) detected by real-time RT-PCR (the lower the number the greater the amount of RNA) in the various formalin-fixed, paraffin-wax embedded (FFPE) and frozen tissue samples (where stated) and the corresponding results for immunohistochemistry (FFPE only) along with the principal cell type labelled and amount of labelling (0 – 5). UD = undetermined. NA = not applicable.

Tissue	No. of samples	Real-Time rt-PCR mean CT value	Morbillivirus IHC (principal cell type positive, overall score)
Brain stem (frozen)	1	25.2	not applicable
Brain stem	3	32.1	positive (neurones, 3)
Cerebellum	4	Undetected	negative
Trachea	1	23.9	positive (syncytia, 5)
Lung	2	24.4	positive (syncytia, 3)
Heart	1	Undetected	negative
Heart valve	1	Undetected	negative
Heart cyst	1	Undetected	negative
Liver	1	22.4	positive (syncytia, 5)
Stomach	1	24.5	positive (syncytia, 3)
Spleen	1	23.6	positive (syncytia, 5)
Lymph node	3	25.0 (range 23-26)	positive (syncytia, 3)
Kidney	1	24.1	positive (syncytia, 4)
Urinary bladder	1	22.0	positive (syncytia, 4)
Testis	1	26.3	positive (UD, 1)
Skin (frozen)	1	40.2	NA
Skin	1	Undetected	positive (syncytia, 2)